SLAC-PUB-17202

Supersymmetric Properties of Hadron Physics from Light-Front Holography and Superconformal Algebra and other Advances in Light-Front QCD

Stanley J. Brodsky

Received: date / Accepted: date

Abstract Light-front holography, together with superconformal algebra, the Pauli spinor representation of the conformal group, have provided new insights into the physics of color confinement and the spectroscopy and dynamics of hadrons. As shown by de Alfaro, Fubini and Furlan, a mass scale can appear in the equations of motion without affecting the conformal invariance of the action if one adds a term to the Hamiltonian proportional to the dilatation operator or the special conformal operator. If one applies the procedure of de Alfaro et al. to the frame-independent light-front Hamiltonian, it leads uniquely to a confining $q\bar{q}$ potential $\kappa^4\zeta^2$, where ζ^2 is the light-front radial variable related in momentum space to the $q\bar{q}$ invariant mass. The same result, including spin terms, is obtained using light-front holography – the duality between the front form and AdS_5, the space of isometries of the conformal group – if one modifies the action of AdS_5 by the dilaton $e^{\kappa^2 z^2}$ in the fifth dimension z. When one generalizes this procedure using superconformal algebra, the resulting light-front eigensolutions lead to a a unified Regge spectroscopy of meson, baryon, and tetraquarks, including supersymmetric relations between their masses and their wavefunctions. One also predicts hadronic light-front wavefunctions and observables such as structure functions, transverse momentum distributions, and the distribution amplitudes. The mass scale κ underlying confinement and hadron masses can be connected to the parameter $\Lambda_{\overline{MS}}$ in the QCD running coupling by matching the nonperturbative dynamics to the perturbative QCD regime. The result is an effective coupling $\alpha_s(Q^2)$ defined at all momenta. The matching of the high and low momentum transfer regimes determines a scale Q_0 which sets the interface between perturbative and nonperturbative hadron dynamics. I also discuss a number of applications of light-front phenomenology.

Keywords Light-Front Holography · QCD · Superconformal Algebra

SLAC National Accelerator Laboratory, Stanford University, Stanford, CA 94309, USA
E-mail: sjbth@slac.stanford.edu

This material is based upon work supported by the U.S. Department of Energy, Office of Science, under Contract No. DE-AC02-76SF00515.

1 Introduction

A central problem in hadron physics is to obtain a color-confining, first approximation to QCD which can predict both the hadron spectrum and the frame-independent light-front wavefunctions underlying hadron phenomenology. The QCD Lagrangian with zero quark mass has no explicit mass scale; the classical theory is conformally invariant. A profound question is then to understand how the proton mass and other hadronic mass scales – the mass gap – can arise even when $m_q = 0$. In fact, chiral QCD has no knowledge of units such as MeV. Since the mass scale is not set by QCD, only ratios of masses are determined, and the theory has dilation invariance. In a sense, chiral QCD has an "extended conformal invariance." However, a remarkable principle, first demonstrated by de Alfaro, Fubini and Furlan (dAFF) [1] in $1+1$ quantum mechanics, is that a mass scale can appear in a Hamiltonian without affecting the conformal invariance of the action. The essential step is to add to the conformal Hamiltonian H_0 terms proportional to the dilation operator D and the special conformal operator K. Confinement appears for all choices if the coefficient of the resulting harmonic oscillator potential is positive. The coefficients introduce the mass scale κ, and the result is $H = H_0 + V$, where V a harmonic oscillator potential $V(x) = \kappa^2 x^2$. The action remains conformal when one changes to a new time variable. The new time variable has finite support, conforming to the fact that the time interval between interactions with confined constituents is finite.

De Téramond, Dosch, and I [2] have shown that a mass gap and a fundamental color confinement scale also appear when one extends the dAFF procedure to light-front (LF) Hamiltonian theory in physical 3+1 spacetime. In the case of mesons, one can convert the full LF Hamiltonian to an effective $q\bar{q}$ valence state Hamiltonian by systematically eliminating the higher Fock states. Remarkably, the resulting light-front potential has a unique form of a harmonic oscillator $\kappa^4\zeta^2$ in the LF equation of motion. The light-front invariant variable is ζ where $\zeta^2 = b_\perp^2 x(1-x)$ is conjugate to the invariiant mass squared $\frac{k_\perp^2}{x(1-x)}$ for massless quarks. The result is a single-variable frame-independent relativistic equation of motion for $q\bar{q}$ bound states, a "Light-Front Schrödinger Equation" [3], analogous to the nonrelativistic radial Schrödinger equation in quantum mechanics. The same result, including spin terms, is obtained using light-front holography – the duality between the front form and AdS_5, the space of isometries of the conformal group – if one modifies the action of AdS_5 by the dilaton $e^{\kappa^2 z^2}$ in the fifth dimension z. An essential point is that the mass scale κ is not determined absolutely by QCD – only ratios of masses are predicted.

The central reason why the mathematical Anti-deSitter space in five dimensions is relevant to hadron physics is that AdS_5 space provides a geometrical representation of the conformal group. Furthermore, AdS_5 is holographically dual to $3+1$ spacetime at fixed light-front time $\tau = t + z/c$. The holographic dictionary is summarized in Fig. 1 Color-confining light-front equations for

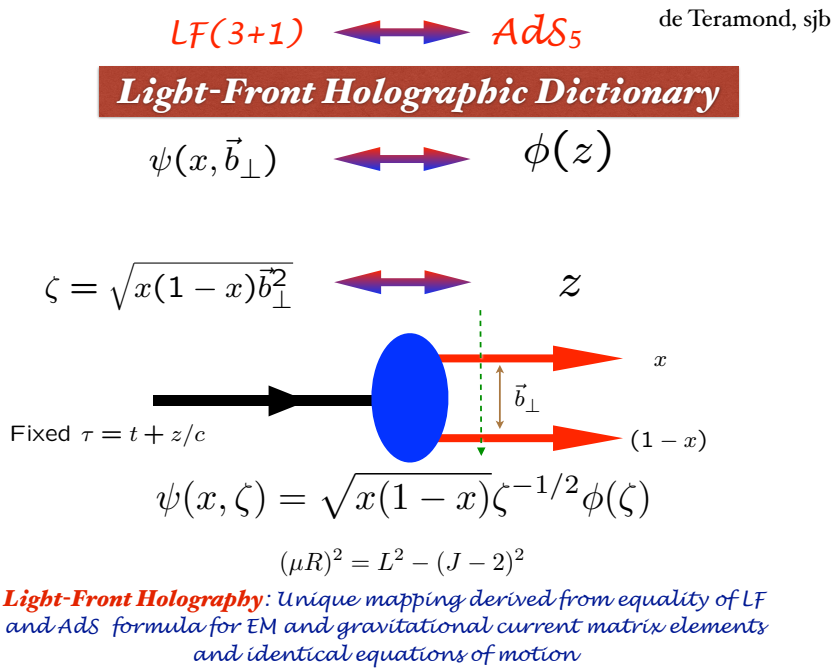

Fig. 1 The holographic dictionary which maps the fifth dimension variable z of the five-dimensional AdS_5 space to the LF radial variable ζ where $\zeta^2 = b_\perp^2(1-x)$. The same physics transformation maps the AdS_5 and $(3+1)$ LF expressions for electromagnetic and gravitational form factors to each other. From Ref. [4]

mesons of arbitrary spin J can be derived [4] from the holographic mapping of the "soft-wall model" modification of AdS_5 space for the specific dilaton profile $e^{+\kappa^2 z^2}$, where one identifies the fifth dimension coordinate z with the light-front coordinate ζ where $\zeta^2 = b_\perp^2 x(1-x)$. The orbital angular momentum quantum number L in the LF theory can be matched to the AdS_5 variable μR by matching the respective equations of motion and the twist dimension of the eigensolutions. Note that $L = max|L^z|$ and there are $2L+1$ degenerate states. This point is discussed for arbitrary spin for mesons and baryons in Ref. [4]. As discussed in section XXX, it also predicts the analytic form of the QCD running coupling in the nonperturbative domain. Further references and reviews of *Light-Front Holography* may be found in refs. [5–9]

The combination of light-front dynamics, its holographic mapping to AdS_5 space, and the dAFF procedure provides new insight into the physics underlying color confinement, the nonperturbative QCD coupling, and the QCD mass scale. A comprehensive review is given in Ref. [8]. The $q\bar{q}$ mesons and their valence LF wavefunctions are the eigensolutions of the frame-independent relativistic bound state LF Schrödinger equation. The mesonic $q\bar{q}$ bound-state eigenvalues for massless quarks are $M^2(n,L,S) = 4\kappa^2(n+L+S/2)$. The equa-

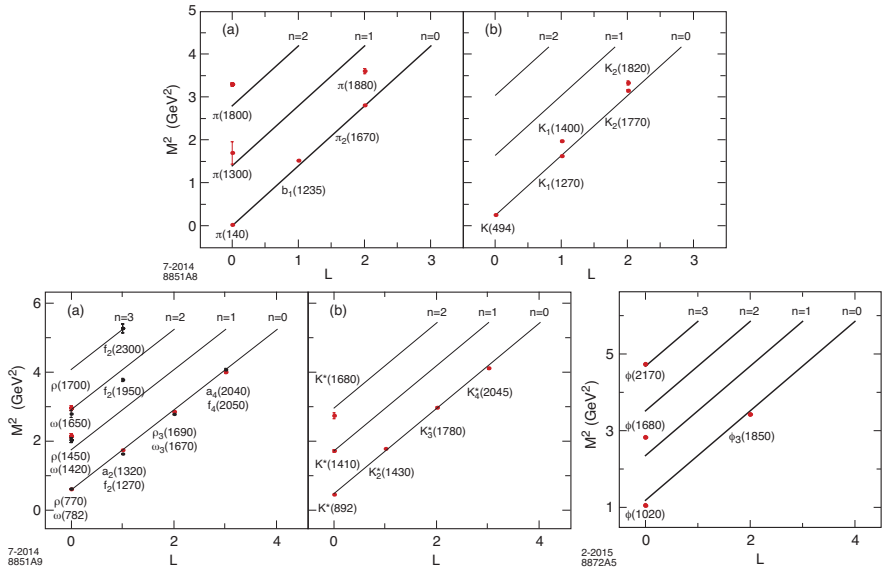

Fig. 2 Comparison of the AdS/QCD prediction $M^2(n, L, S) = 4\kappa^2(n + L + S/2)$ for the orbital L and radial n excitations of the meson spectrum with experiment. The pion is predicted to be massless for zero quark mass. The u, d, s quark masses can be taken into account by perturbing in $< m_q^2/x >$. The fitted value of $\kappa = 0.59$ GeV for pseudoscalar mesons, and $\kappa = 0.54$ GeV for vector mesons.

tion predicts that the pion eigenstate $n = L = S = 0$ is massless at zero quark mass. The Regge spectra of the pseudoscalar $S = 0$ and vector $S = 1$ mesons are predicted correctly, with equal slope in the principal quantum number n and the internal orbital angular momentum L. A comparison with experiment is shown in Fig. 2.

It is interesting to note that the contribution of the *'H'* diagram to $Q\bar{Q}$ scattering is IR divergent as the transverse separation between the Q and the $\bar{Q}$ increases [10]. This is a signal that pQCD is inconsistent without color confinement. The sum of such diagrams could sum to the confinement potential $\kappa^4\zeta^2$ dictated by the dAFF principle that the action remains conformally invariant despite the appearance of the mass scale κ in the Hamiltonian. The $\kappa^4\zeta^2$ confinement interaction between a q and $\bar{q}$ will induce a κ^4/s^2 correction to $R_{e^+e^-}$, replacing the $1/s^2$ signal usually attributed to a vacuum gluon condensate.

The predicted hadronic LFWFs are functions of the LF kinetic energy $\mathbf{k}_\perp^2/x(1-x)$ – the conjugate of the LF radial variable $\zeta^2 = b_\perp^2 x(1-x)$ – times a function of $x(1-x)$; they do not factorize as a function of $\mathbf{k}_\perp^2$ times

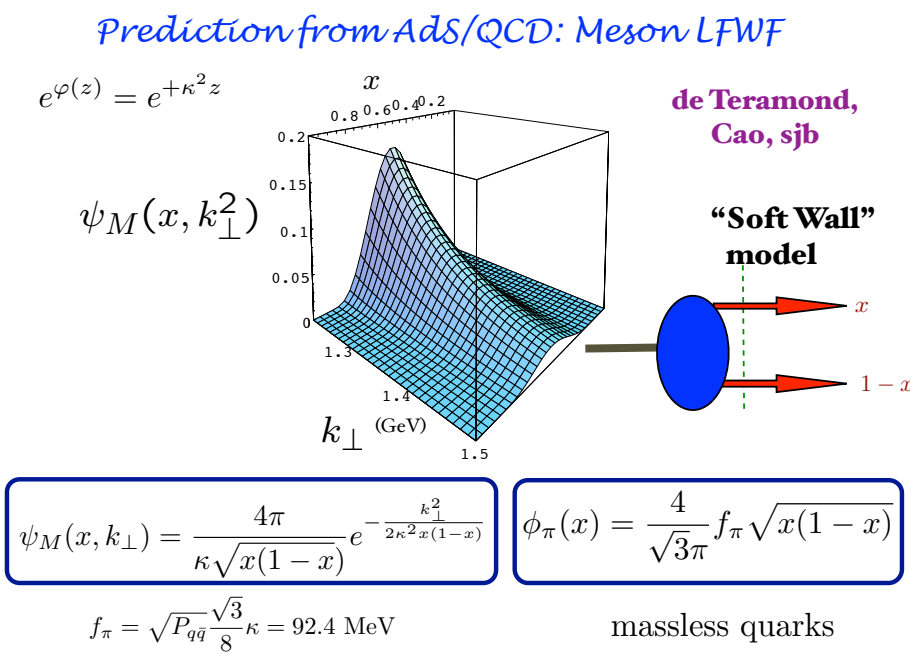

Fig. 3 Prediction from AdS/QCD and Light-Front Holography for meson LFWFs $\psi_M(x, \mathbf{k}_\perp)$ and the pion distribution amplitude.

a function of x. The resulting nonperturbative pion distribution amplitude $\phi_\pi(x) = \int d^2\mathbf{k}_\perp \psi_\pi(x, \mathbf{k}_\perp) = (4/\sqrt{3}\pi) f_\pi \sqrt{x(1-x)}$, see Fig. 3, which controls hard exclusive process, is consistent with the Belle data for the photon-to-pion transition form factor [11]. The AdS/QCD light-front holographic eigenfunction for the ρ meson LFWF $\psi_\rho(x, \mathbf{k}_\perp)$ gives excellent predictions for the observed features of diffractive ρ electroproduction $\gamma^* p \to \rho p'$, as shown by Forshaw and Sandapen [12]

LF holography gives a remarkable first approximation to hadron spectroscopy and the hadronic LFWFs. A new method for solving nonperturbative QCD "Basis Light-Front Quantization" (BLFQ) [13], uses the eigensolutions of a color-confining approximation to QCD (such as LF holography) as the basis functions, rather than the plane-wave basis used in DLCQ, thus incorporating the full dynamics of QCD. LFWFs can also be determined from the covariant Bethe-Salpeter wavefunction by integrating over k^- [14].

2 Superconformal Algebra

The Light-Front Schrödinger Equation derived from LF holography incorporates color confinement and other essential spectroscopic and dynamical fea-

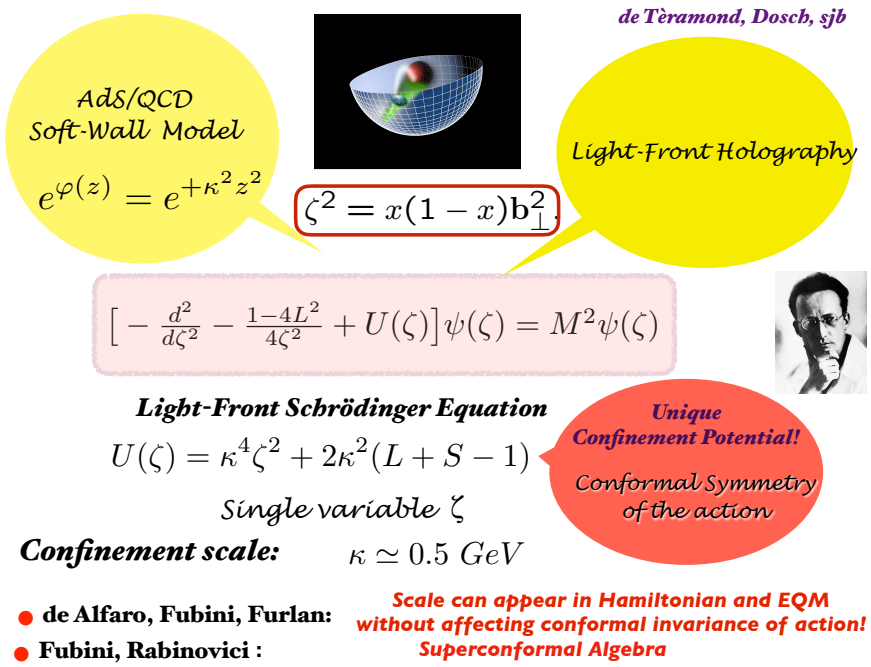

Fig. 4 The convergence of theoretical methods for generating a model of hadron spectroscopy and dynamics with color confinement and meson-baryon supersymmetric relations.
.

tures of hadron physics, including a massless pion for zero quark mass and linear Regge trajectories with the same slope in the radial quantum number n and internal orbital angular momentum L. When one generalizes this procedure using *superconformal algebra*, the resulting light-front eigensolutions predict a unified Regge spectroscopy of meson, baryon, and tetraquarks, including remarkable supersymmetric relations between the masses of mesons and baryons of the same parity.

The synthesis of AdS/QCD with superconformal algebra and the dAFF ansatz is illustrated in Fig. 4

The QCD Lagrangian is not supersymmetrical; however its hadronic eigensolutions conform to a fundamental 4-plet supersymmetric representation of superconformal algebra, reflecting the underlying conformal symmetry of semiclassical QCD for massless quarks. The conformal group has an elegant 2×2 Pauli matrix representation called superconformal algebra, originally discovered by Haag, Lopuszanski, and Sohnius [15](1974) The conformal Hamiltonian operator and the special conformal operators can be represented as anticommutators of Pauli matrices $H = 1/2[Q, Q^\dagger]$ and $K = 1/2[S, S^\dagger]$. As shown by Fubini and Rabinovici, [16], a nonconformal Hamiltonian with a mass scale and universal confinement can then be obtained by shifting $Q \to Q + \omega K$, the

analog of the dAFF procedure. In effect one has obtained generalized supercharges of the superconformal algebra [16].

This approach predicts novel supersymmetric relations between mesons, baryons, and tetraquarks of the same parity as members of the same 4-plet representation of superconformal algebra. The 4-plet representation illustrated in Fig. 2 not only implies identical masses for the bosonic and fermionic hadron eigenvalues, but also supersymmetric relations between their eigenfunctions– their light-front wavefunctions. The baryonic eigensolutions correspond to bound states of 3_C quarks to a $\bar{3}_C$ spin-0 or spin-1 diquark cluster; the tetraquarks in the 4-plet are bound states of diquarks and anti-diquarks.

The 4-plet contains two entries $\Psi^{\pm}$ for each baryons corresponding to internal orbital angular momentum $L$and $L+1$. This is the analog of the eigensolution of the Dirac-Coulomb equation which lower components $\Psi^- = \frac{\boldsymbol{\sigma}\cdot\mathbf{p}}{m+E-V}\Psi^+$ In the case of a nucleon, the overlap of the $L = 0$ and $L = 1$ LF wavefunctions in the Drell-Yan-West formula is required to have a non-zero Pauli form factor $F_2(Q^2)$ and anomalous magnetic moment [17]. The existence of both components is also necessary to generate the pseudo-T-odd Sivers single-spin asymmetry in deep inelastic lepton-nucleon scattering [87].

Superconformal algebra also predicts universal Regge-slopes in n and L for mesons: $M^2(n, L) = 4\kappa^2(n + L)$ for mesons and $M^2(n, L) = 4\kappa^2(n + L + 1)$ for baryons, consistent with observed hadronic spectroscopy. The pion eigenstate with $(n = L = S = 0)$ thus has zero mass in the chiral $m_q \to 0$ limit. The predicted meson, baryon and tetraquark masses are identical if one identifies a meson with internal orbital angular momentum L_M with its superpartner baryon or tetraquark with $L_B = L_M - 1$. An example of the mass degeneracy of ρ/ω meson Regge trajectory with the $J = 3/2$ Δ-baryon trajectory is shown in Fig. **??**. The combination of light-front holography with superconformal algebra thus leads to the novel prediction that hadron physics has supersymmetric properties in both spectroscopy and dynamics.

The LF Schrödinger Equations for baryons and mesons derived from superconformal algebra are shown in Fig. 6. In effect the baryons on the proton (Delta) trajectory are bound states of a quark with color 3_C and scalar (vector) diquark with color $\bar{3}_C$ The proton eigenstate labeled ψ^+ (parallel quark and baryon spins) and ψ^- (anti parallel quark and baryon spins) have equal Fock state probability – a feature of "quark chirality invariance". Predictions for the static properties of the nucleons are discussed in Ref. [22]

The supersymmetry of the 4-plet representation is also exhibited dynamically in terms of common features of the light-front wavefunctions of mesons, baryons, and tetraquarks. One can test the similarities of their wavefunctions and form factors in exclusive reactions such as $e^+e^- \to \pi T$ where T is a tetraquark [23].

Empirically viable predictions for spacelike and timelike hadronic form factors, structure functions, distribution amplitudes, and transverse momentum distributions have been obtained [24]. One can also observe features of superconformal symmetry in the spectroscopy of heavy-light mesons and baryons.

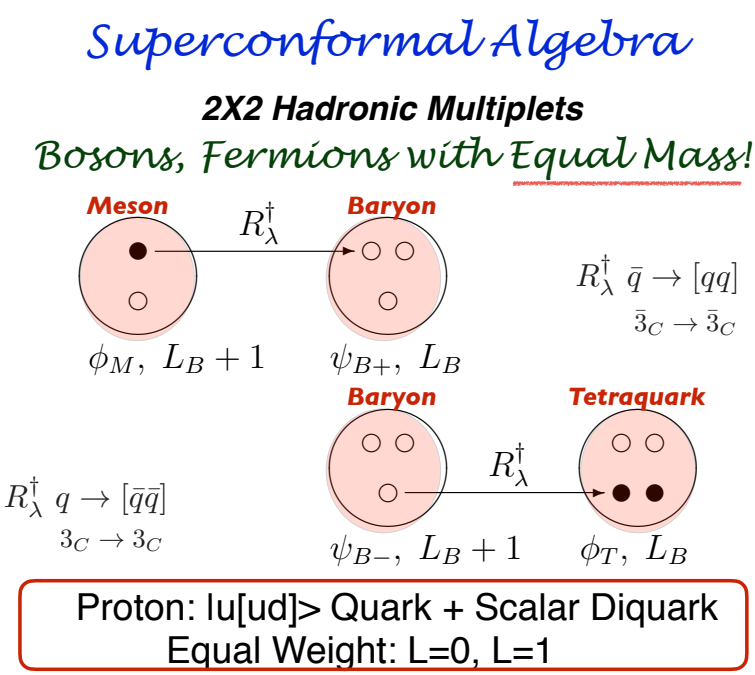

Fig. 5 The 4-plet representation of mass-degenerate hadronic states predicted by superconformal algebra [2]. Mesons are $q\bar{q}$ bound states, baryons are quark plus anti-diquark bound states and tetraquarks are diquark plus antidiquark bound states. The supersymmetric ladder operator $R_\lambda^\dagger$ connects quarks and anti-diquark clusters of the same color. The baryons have two Fock states with orbital angular momentum L_B and L_B+1 with equal weight. The predicted meson, baryon and tetraquark masses are identical if one identifies a meson with internal orbital angular momentum L_M with its superpartner baryon or tetraquark with $L_B = L_M - 1$.

Superconformal QM and its holographic embedding itself does not incorporate longitudinal x^- dynamics. However. The inclusion of the quark masses through the invariant mass is an extension of the model. The solutions In momentum space are then Gaussian in $\mathcal{M}^2 = \frac{\mathbf{k}_\perp{}^2+m^2}{x(1-x)}$. This is proportional to the $\frac{\mathbf{p}^2}{2m_r}$ kinetic energy in the nonrelativistic limit where m_r is the reduced mass. The resulting LF potential thus confines in all three spatial directions.

3 Light-Front QCD

When one makes a measurement such as Compton scattering on the proton $\gamma p\to\gamma' p'$ or lepton-proton scattering $\ell p\to\ell' X$ the hadron is observed along the light-front (LF) (transverse to the light cone) at a fixed time $\tau = x^+ = x^3/c + x^0$ – not at a fixed "instant" time t. This is the underlying principle of

LF Holography **Baryon Equation**

$$\Big(-\partial_\zeta^2+\kappa^4\zeta^2+2\kappa^2(L_B+1)+\frac{4L_B^2-1}{4\zeta^2}\Big)\psi_J^+=M^2\psi_J^+ \quad \text{G22}$$

$$\Big(-\partial_\zeta^2+\kappa^4\zeta^2+2\kappa^2 L_B+\frac{4(L_B+1)^2-1}{4\zeta^2}\Big)\psi_J^-=M^2\psi_J^- \quad \text{G11}$$

$$M^2(n,L_B)=4\kappa^2(n+L_B+1)$$

S=1/2, P=+

both chiralities

Meson Equation

$$\Big(-\partial_\zeta^2+\kappa^4\zeta^2+2\kappa^2(J-1)+\frac{4L_M^2-1}{4\zeta^2}\Big)\phi_J=M^2\phi_J \quad \text{G11}$$

$$M^2(n,L_M)=4\kappa^2(n+L_M)$$

Same κ !

S=0, I=1 Meson is superpartner of S=1/2, I=1 Baryon

Meson-Baryon Degeneracy for $L_M=L_B+1$

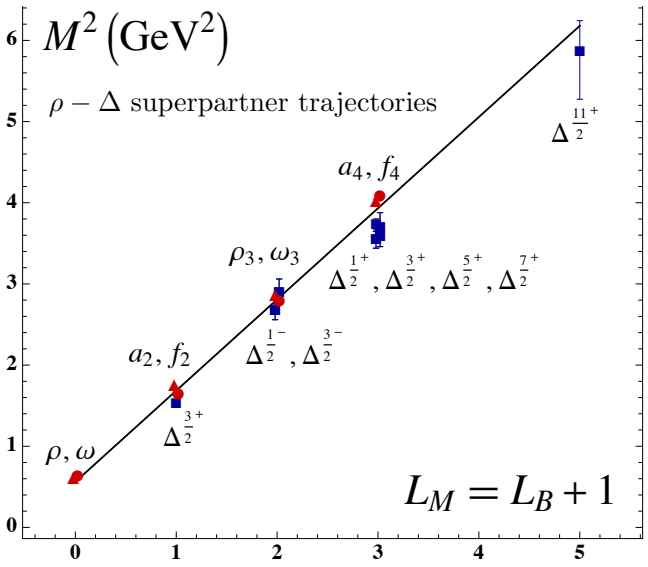

Fig. 6 (A). The LF Schrödinger equations for baryons and mesons for zero quark mass derived from the Pauli 2×2 matrix representation of superconformal algebra. The $\psi^{\pm}$ are the baryon quark-diquark LFWFs where the quark spin $S_q^z=\pm 1/2$ is parallel or antiparallel to the baryon spin $J^z=\pm 1/2$. The meson and baryon equations are identical if one identifies a meson with internal orbital angular momentum L_M with its superpartner baryon with $L_B = L_M - 1$. See Refs. [19–21]. (B). Comparison of the ρ/ω meson Regge trajectory with the $J = 3/2$ Δ baryon trajectory. Superconformal algebra predicts the degeneracy of the meson and baryon trajectories if one identifies a meson with internal orbital angular momentum L_M with its superpartner baryon with $L_M = L_B + 1$. See Refs. [19,20].

the "front form" discussed by Dirac [25]. The LF time τ reduces to ordinary time at $c \to \infty$.

The LF-time evolution operator is $P^- = P^0 - P^3 = i\frac{d}{dx^+}$. Since $P^+ = P^0 + P^3$ and $P^\perp$ are kinematical, one can define the LF Hamiltonian $H_{LF} = P^+P^- - P_\perp^2$. In the case of QCD, the eigenvalues of the LF invariant Hamiltonian H_{LF}^{QCD} are the squares of the hadron masses M_H^2: $H_{LF}^{QCD}|\Psi_H >= M_H^2|\Psi_H >$ [26], and the eigensolutions of H_{LF}^{QCD} provide the n-particle hadronic LF Fock state wavefunctions (LFWFs) $\psi_n^H(x_i, \mathbf{k}_{\perp i}, \lambda_i) =< n|\Psi_H >$, the projection on the free Fock basis. The constituents' physical momenta are $p_i^+ = x_i P^+$, and $\mathbf{p}_{\perp i} = x_i \mathbf{P}_\perp + \mathbf{k}_{\perp i}$ where $\sum_{i=1}^n x_i = 1$ and $\sum_{i=1}^n \mathbf{k}_{\perp i} = \mathbf{0}$. The λ_i label the spin projections S_i^3. The total angular momentum is conserved: $J^3 = \sum_{i=1}^n S_i^3 + \sum_{i=1}^{n-1} L_i^3$ for every Fock state. One can derive H_{LF} directly from the QCD Lagrangian and avoid ghosts and longitudinal gluonic degrees of freedom by choosing to work in the light-front gauge $A^+ = 0$. Physical results however, are independent of the gauge choice, as well as conventions such as the choice of renormalization scheme or the choice of the initial renormalization scale.

The LFWFs are Poincare' invariant; i.e., they are boost invariant, independent of the hadron's P^+ and $P_\perp$ and they are thus independent of the motion of the hadron or observer. This is analogous to the fact that the image made by a flash photograph is independent of the velocity of camera. Since the LFWFs are independent of the hadron's momentum, there is no length contraction. The physical properties of a hadron are independent of the observer's Lorentz frame. The absence of length contraction in the front form was first noted by Terrell [27] and Penrose [28]. One thus measures the same structure function in an electron-ion collider as in an electron-scattering experiment where the target hadron is at rest.

In the case of QCD, the eigenvalues of the LF invariant Hamiltonian $H_{LF} = P^+P^- - \mathbf{P}_\perp^2$, where $P^+ = P^0 + P^z$ and $\mathbf{P}_\perp$ are kinematical, are the squares of the hadron masses M_H^2: $H_{LF}|\Psi_H >= M_H^2|\Psi_H >$ [26]. The eigensolutions of H_{LF} provide the n-particle hadronic LF Fock state wavefunctions (LFWFs) $\psi_n^H(x_i, \mathbf{k}_{\perp i}, \lambda_i) =< n|\Psi_H >$, the projection on the free Fock basis. The LF Hamiltonian, can be derived directly from the QCD Lagrangian. The constituents' physical momenta are $p_i^+ = x_i P^+$, and $\mathbf{p}_{\perp i} = x_i \mathbf{P}_\perp + \mathbf{k}_{\perp i}$, and the λ_i label the spin projections S_i^z.

The LF Hamiltonian H_{LF}^{QCD}, can be derived directly from the QCD Lagrangian. One can avoid ghosts and longitudinal gluonic degrees of freedom by choosing the light-front gauge $A^+ = 0$. Physical results however, are independent of the gauge choice, as well as conventions such as the choice of renormalization scheme or the choice of the initial renormalization scale. One then can write $H_{LF}^{QCD} = H_{LFKE}^{QCD} + H_{LFPE}^{QCD}$ where the LF kinetic energy $H_{LFKE}^{QCD} = \sum_i \frac{\mathbf{k}_{\perp \mathbf{i}}^2 + \mathbf{m}_\mathbf{i}^2}{\mathbf{x}_\mathbf{i}}$ is equal to the invariant mass squared $\mathcal{M}_n^2 = \sum_i^n p_i^\mu \sum_i^n p_{\mu i}$ of the free constituents of the n-particle Fock state. The quark masses appear in the LF kinetic energy as $\sum_i^n \frac{m_{qi}^2}{x_i}$. This contribution can be derived from the Higgs theory quantized using LF dynamics. The confined quark field ψ_q

couples to the background Higgs field $g_{\overline{\Psi}_q} < H > \Psi_q$ via its Yukawa scalar matrix element coupling $g_q < H > \bar{u}(p)1u(p) = m_q \times \frac{m_q}{x} = \frac{m^2}{x}$.

4 The QCD Coupling at all Scales

The QCD running coupling $\alpha_s(Q^2)$ sets the strength of the interactions of quarks and gluons as a function of the momentum transfer Q. The dependence of the coupling Q^2 is needed to describe hadronic interactions at both long and short distances. The QCD running coupling can be defined [29] at all momentum scales from a perturbatively calculable observable, such as the coupling $\alpha^s_{g_1}(Q^2)$, which is defined from measurements of the Bjorken sum rule. At high momentum transfer, such "effective charges" satisfy asymptotic freedom, obey the usual pQCD renormalization group equations, and can be related to each other without scale ambiguity by commensurate scale relations [30].

The dilaton $e^{+\kappa^2 z^2}$ soft-wall modification of the AdS_5 metric, together with LF holography, predicts the functional behavior of the running coupling in the small Q^2 domain [31]: $\alpha^s_{g_1}(Q^2) = \pi e^{-Q^2/4\kappa^2}$. Measurements of $\alpha^s_{g_1}(Q^2)$ are remarkably consistent [32] with this predicted Gaussian form; the best fit gives $\kappa = 0.513 \pm 0.007\ GeV$. See Fig. 7 Deur, de Teramond, and I [31,33, 34] have also shown how the parameter κ, which determines the mass scale of hadrons and Regge slopes in the zero quark mass limit, can be connected to the mass scale Λ_s controlling the evolution of the perturbative QCD coupling. The high momentum transfer dependence of the coupling $\alpha_{g1}(Q^2)$ is predicted by pQCD. The matching of the high and low momentum transfer regimes of $\alpha_{g1}(Q^2)$ – both its value and its slope – then determines a scale $Q_0 = 0.87 \pm 0.08$ GeV which sets the interface between perturbative and nonperturbative hadron dynamics. This connection can be done for any choice of renormalization scheme, such as the $\overline{MS}$ scheme, as seen in Fig. 7. The result of this perturbative/nonperturbative matching is an effective QCD coupling defined at all momenta. A remarkably similar result, a "process-independent running coupling" has been derived using alternative methods has recently been derived in Ref. [35].

The predicted value of $\Lambda_{\overline{MS}} = 0.339 \pm 0.019\ GeV$ from this analysis agrees well the measured value [36] $\Lambda_{\overline{MS}} = 0.332 \pm 0.019\ GeV$. These results, combined with the AdS/QCD superconformal predictions for hadron spectroscopy, allow us to compute hadron masses in terms of $\Lambda_{\overline{MS}}$: $m_p = \sqrt{2}\kappa = 3.21\ \Lambda_{\overline{MS}}$, $m_\rho = \kappa = 2.2\ \Lambda_{\overline{MS}}$, and $m_p = \sqrt{2} m_\rho$, meeting a challenge proposed by Zee [37]. The value of Q_0 can be used to set the factorization scale for DGLAP evolution of hadronic structure functions and the ERBL evolution of distribution amplitudes. Deur, de Téramond, and I have also computed the dependence of Q_0 on the choice of the effective charge used to define the running coupling and the renormalization scheme used to compute its behavior in the perturbative regime. The use of the scale Q_0 to resolve the factorization scale uncertainty in structure functions and fragmentation functions, in combination with the scheme-indepedent *principle of maximum sensitivity* (PMC) [38] for setting

renormalization scales, can greatly improve the precision of pQCD predictions for collider phenomenology.

5 Applications

The combination of light-front holography and superconformal algebra provide new insights into the structure of hadrons in terms of their frame-independent light-front wavefunctions. For example, hadron structure functions such as $F_2(x, Q^2)$ measured in deep inelastic lepton-scattering and the transverse momentum distributions measured in deeply virtual Compton scattering can be computed from the squares of the LFWFs. See e.g., ref. [39]. The AdS/QCD solutions provide the nonperturbative input for $Q^2 < Q_0^2$. At higher $Q^2 > Q_0^2$, structure functions evolve according to DGLAP evolution. The renormalization scale entering the running couping in DGLAP evolution can be set unambiguously and without scheme dependence using the *Principle of Maximum Conformality* [38].

Exclusive hadron amplitudes, such as the spacelike elastic and transition form factors are also given in terms of convolutions of light-front wavefunctions [17]. Hadronic scattering amplitudes involving quark interchange such $K^+p \to K^+p$ scattering can be written in terms of the product of four LFWFs [40]. In each case, the dimensional counting rules are obeyed. At high momentum transfer, exclusive amplitudes factorize as the product of hard quark and gluon subprocess amplitudes convoluted with the hadronic distribution amplitudes $\psi_H(x_i, Q)$ which are obtained by integrating the LFWFs over transverse momentum $k_{\perp i}^2 < Q^2$. The AdS/QCD solutions provide the nonperturbative input for $Q^2 < Q_0^2$. At higher $Q^2 > Q_0^2$, the distribution amplitudes evolve according to ERBL evolution. For example, the nonperturbative pion distribution amplitude is $\phi_\pi(x) = \int d^2\mathbf{k}_\perp \psi_\pi(x, \mathbf{k}_\perp) = (4/\sqrt{3}\pi) f_\pi \sqrt{x(1-x)}$, which controls hard exclusive process, is consistent with the Belle data for the photon-to-pion transition form factor [11]. See Fig. 3. The meson distribtion amplitude evolves to $x(1-x)$ at $Q^2 \to \infty$. In the case of the deuteron, ERBL evolution leads to "hidden color" Fock state contributions [41]. The AdS/QCD light-front holographic eigenfunction for the ρ meson LFWF $\psi_\rho(x, \mathbf{k}_\perp)$ gives excellent predictions for the observed features of diffractive ρ electroproduction $\gamma^* p \to \rho p'$, as shown by Forshaw and Sandapen [12]

It should be noted that The hadronic LFWFs from AdS/QCD are functions of the LF kinetic energy $\mathbf{k}_\perp^2/x(1-x)$ – the conjugate of the LF radial variable $\zeta^2 = b_\perp^2 x(1-x)$ – times a function of $x(1-x)$; they do not factorize as a function of $\mathbf{k}_\perp^2$ times a function of x.

5.1 Other applications

1. *Hadronization at the Amplitude Level* The new insights into color confinement given by AdS/QCD and superconformal algebra suggest that one

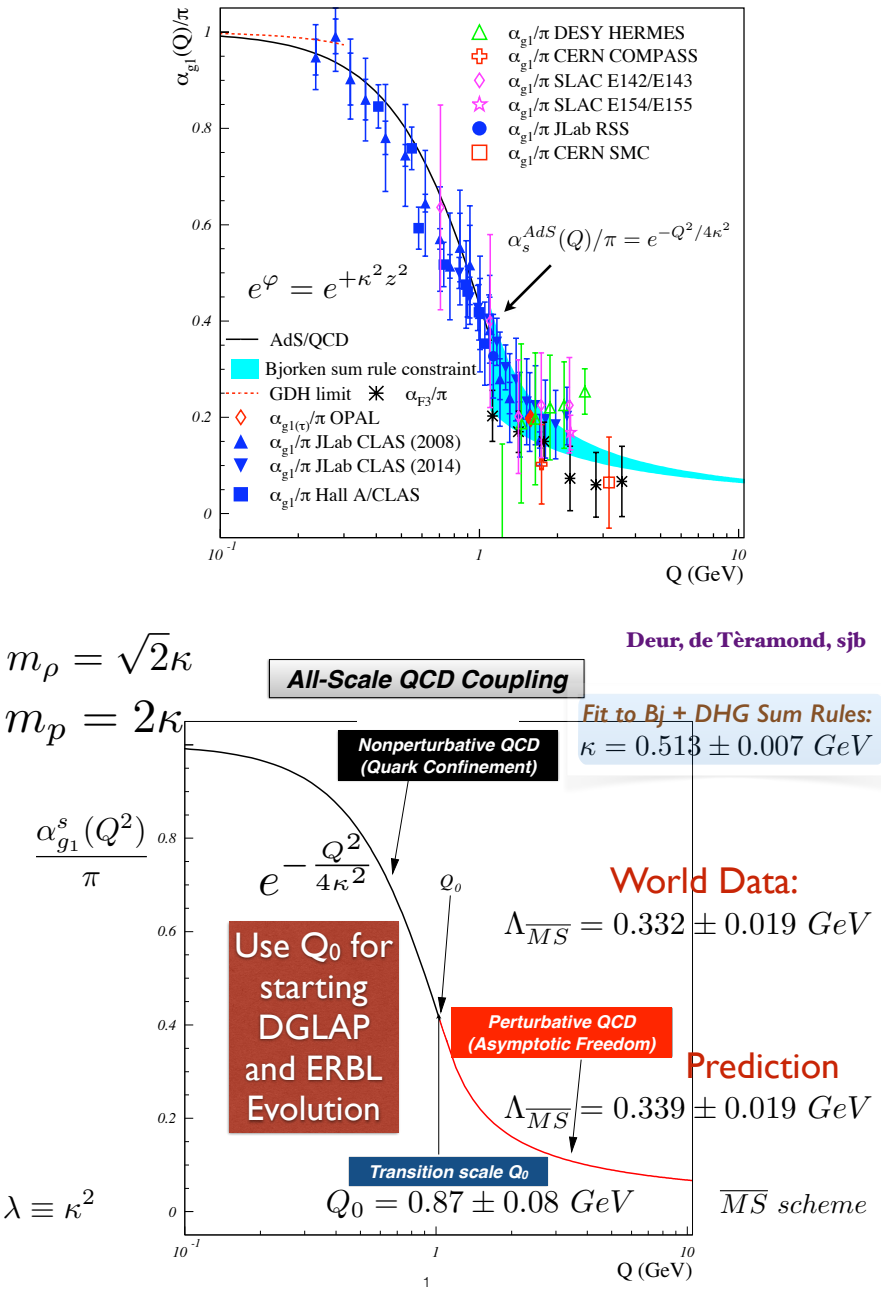

Fig. 7 (A) Comparison of the predicted nonpertubative coupling, based on the dilaton $\exp(+\kappa^2 z^2)$ modification of the AdS_5 metric, with measurements of the effective charge $\alpha^s_{g_1}(Q^2)$, as defined from the Bjorken sum rule. (B) Prediction from LF Holography and pQCD for the QCD running coupling $\alpha^s_{g_1}(Q^2)$ at all scales. The magnitude and derivative of the perturbative and nonperturbative coupling are matched at the scale Q_0. This matching connects the perturbative scale $\Lambda_{\overline{MS}}$ to the nonpertubative scale κ which underlies the hadron mass scale. See Ref. [34].

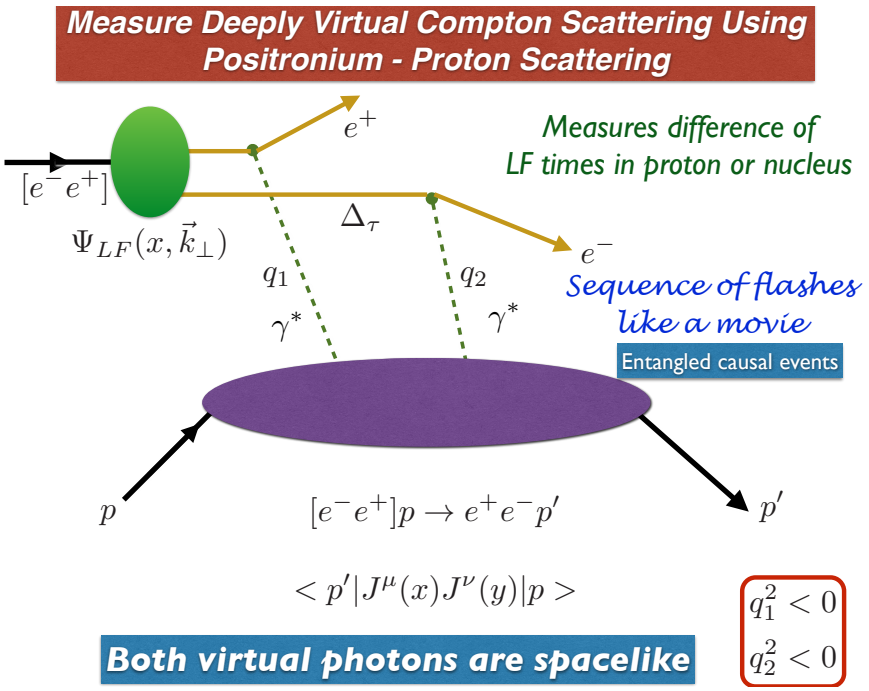

Fig. 8 Doubly Virtual Compton scattering on a proton (or nucleus) can be measured for two *spacelike* photons $q_1^2, q_2^2 < 0$ with minimal, tunable, skewness ξ using positronium-proton scattering $[e^+e^-]p \to e^+e^-p'$.

could compute hadronization at amplitude level [42] using the confinement interaction and the LFWFs predicted by AdS/QCD and Light-Front Holography. The invariant mass of a color-singlet cluster $\mathcal{M}$ is the key variable which separates perturbative and nonperturbative dynamics. For example, consider e^+e^- annihilation using LF τ - ordered perturbation theory. At an early stage in LF time the annihilation will produce jets of quarks and gluons in an intermediate state that are off the P^- energy shell. If a color-singlet cluster of partons in a jet satisfies $\mathcal{M}^2 < \kappa^2$, the cluster constituents will be ruled by the $\kappa^4\zeta^2$ color-confinement potential. At this stage, the LFWF ψ_H converts the off-shell partons to the on-shell hadron. Quarks and gluons only appear in intermediate states, but only hadrons can be produced. Thus the AdS/QCD Light-Front Holographic model suggests how one can implement the transition between perturbative and nonperturbative QCD. For a QED analog, see Refs. [43,44].

2. *Direct Higher Twist Processes* Higher-twist subprocesses such as $qq \to p\bar{q}$ and $gq \to \pi q$ where the hadron is produced directly in the hard-scattering reaction are also predicted by QCD. Such direct processes produce a hadron without the usual same-side hadronic energy produced from quark or gluon jet fragmentation This effect is similar to 'direct photon' production from a

$gq \to \gamma q$ subprocess. The absence of same side hadrons has been observed at RHIC [45]. If a hadron is produced directly in the hard subprocess, it is color transparent and suffers minimal absorption in a nuclear reaction. This can account for the "baryon anomaly" – the high baryon-to-meson ratio observed in central nucleus-nucleus collisions at high p_T [46]. The rate for direct hadron processes is amplified by the fact that the initial partons are produced with minimum x_1 and x_2 where the structure functions are maximized. The hard subprocess energy $\hat{s} = x_1 x_2 s$ is converted to the production of high p_T hadron with maximum efficiency. The fast power-law fall-off observed at fixed x_T at the ISR and the Cronin et al. Chicago-Princeton experiments at Fermilab [47] have a natural explanation in terms such processes. For a review, see [48].

3. *Ridge formation from flux-tube collisions* In the case of $ep \to e'X$, one can consider the collisions of the confining QCD flux tube appearing between the q and $\bar{q}$ of the virtual photon with the flux tube between the quark and diquark of the proton. Since the $q\bar{q}$ plane is aligned with the scattered electron's plane, the resulting "ridge" of hadronic multiplicity produced from the $\gamma^* p$ collision will also tend to be aligned with the scattering plane of the scattered electron. The virtual photon's flux tube will also depend on the photon virtuality Q^2, as well as the flavor of the produced pair arising from $\gamma^* \to q\bar{q}$. In the case of high energy $\gamma^*\gamma^*$ collisions, one can control the produced hadron multiplicity and ridge geometry using the scattered electrons' planes or the scattered proton planes in ultra-peripheral collisions at the LHC. The resulting dynamics [49] is a natural extension of the flux-tube collision description of the ridges produced in $p-p$ collisions [50].
4. *Relativistic Structure of Atoms* The light-front formalism can be applied directly to relativistic atomic physics. For example one can measure the boost-invariant LF wavefunctions of atoms such as positronium and observe the transition from the nonrelativistic Schródinger regime to the full dynamics of QED at short distances. One can produce a relativistic positronium beam using the collisions of laser photons with high energy photons or by measuring Bethe-Heitler pair production just below the e^+e^- threshold. An analogous process will create the "true muonium" atom $[\mu^-\mu^-]$ [43,44]. One can the study the dissociation in a thin target of the relativistic positronia atoms to an electron and positron with light front momentum fractions x and $1-x$ and opposite transverse momenta in analogy to the E791 measurements of the diffractive dissociation of the pion to two jets [51]. The cross section is proportional to the transverse momentum derivative of the LF wavefunction squared. The LFWF of positronium in the relativistic domain has recently been computed using the BLFQ method in ref. [52]. The study of higher LF Fock states such as $|e^+e^-\gamma>$ and $|e^+e^-e^+e^->$ is also possible.
5. *Doubly-Spacelike Virtual Compton Scattering* The amplitude for doubly virtual Compton scattering on a proton $\gamma^*(q_1)p \to \gamma^*(q_2)p'$ (or nucleus) can be measured in positronium-proton elastic scattering where the exchanged photons are *both spacelike* $q_1^2 < 0, q_2^2 < 0$. For example, the in-

coming electron and positron can each scatter with opposite transverse momenta leaving the proton intact with minimum momentum transfer. See Fig.8 The imaginary part of this forward amplitude is proportional by unitarity to $\sigma(gamma^* p \to X)$. One can also measure double deep inelastic scattering $\gamma^*\gamma^* p \to X$, as well as elastic positronium-proton scattering $[e^+e^-]p \to [e^+e^-]'p'$.

Acknowledgments

Presented at Light-Cone 2017, *Frontiers in Light Front Hadron Physics: Theory and Experiment* September 18-22, 2017, Mumbai, Maharashtra, India. I thank Prof. Anuradha Misra and her colleagues for organizing an outstanding conference at the University of Mumbai. The results presented here are based on collaborations and discussions with Kelly Chiu, Alexandre Deur, Guy de Téramond, Guenter Dosch, Marina Nielsen, Fred Goldhaber, Paul Hoyer, Dae Sung Hwang, Rich Lebed, Simonetta Liuti, Cedric Lorce, Matin Mojaza, Michael Peskin, Craig Roberts, Ivan Schmidt, and Xing-Gang Wu. This research was supported by the Department of Energy, contract DE–AC02–76SF00515. SLAC-PUB-17202.

References

1. V. de Alfaro, S. Fubini and G. Furlan, Nuovo Cim. A **34**, 569 (1976).
2. S. J. Brodsky, G. F. de Téramond and H. G. Dosch, Phys. Lett. B **729**, 3 (2014) doi:10.1016/j.physletb.2013.12.044 [arXiv:1302.4105 [hep-th]].
3. G. F. de Téramond and S. J. Brodsky, Phys. Rev. Lett. **102**, 081601 (2009) doi:10.1103/PhysRevLett.102.081601 [arXiv:0809.4899 [hep-ph]].
4. G. F. de Téramond, H. G. Dosch and S. J. Brodsky, Phys. Rev. D **87**, no. 7, 075005 (2013) doi:10.1103/PhysRevD.87.075005 [arXiv:1301.1651 [hep-ph]].
5. G. F. de Téramond and S. J. Brodsky, Nucl. Phys. Proc. Suppl. **199**, 89 (2010) doi:10.1016/j.nuclphysbps.2010.02.010 [arXiv:0909.3900 [hep-ph]].
6. S. J. Brodsky and F. Guy de Téramond, Chin. Phys. C **34**, no. 9, 1229 (2010) doi:10.1088/1674-1137/34/9/015 [arXiv:1001.1978 [hep-ph]].
7. G. F. de Téramond , S. J. Brodsky and H. G. Dosch, EPJ Web Conf. **73**, 01014 (2014) doi:10.1051/epjconf/20147301014 [arXiv:1401.5531 [hep-ph]].
8. S. J. Brodsky, G. F. de Téramond, H. G. Dosch and J. Erlich, Phys. Rept. **584**, 1 (2015) doi:10.1016/j.physrep.2015.05.001 [arXiv:1407.8131 [hep-ph]].
9. S. J. Brodsky, A. Deur, G. F. de Téramond and H. G. Dosch, Int. J. Mod. Phys. Conf. Ser. **39**, 1560081 (2015) doi:10.1142/S2010194515600812 [arXiv:1510.01011 [hep-ph]].
10. A. V. Smirnov, V. A. Smirnov and M. Steinhauser, Phys. Rev. Lett. **104**, 112002 (2010) doi:10.1103/PhysRevLett.104.112002 [arXiv:0911.4742 [hep-ph]].
11. S. J. Brodsky, F. G. Cao and G. F. de Téramond, Phys. Rev. D **84**, 075012 (2011) doi:10.1103/PhysRevD.84.075012 [arXiv:1105.3999 [hep-ph]].
12. J. R. Forshaw and R. Sandapen, Phys. Rev. Lett. **109**, 081601 (2012) doi:10.1103/PhysRevLett.109.081601 [arXiv:1203.6088 [hep-ph]].
13. J. P. Vary, X. Zhao, A. Ilderton, H. Honkanen, P. Maris and S. J. Brodsky, Nucl. Phys. Proc. Suppl. **251-252**, 10 (2014) doi:10.1016/j.nuclphysbps.2014.04.002 [arXiv:1406.1838 [nucl-th]].
14. S. J. Brodsky *et al.*, arXiv:1502.05728 [hep-ph].
15. R. Haag, J. T. Lopuszanski and M. Sohnius, Nucl. Phys. B **88**, 257 (1975). doi:10.1016/0550-3213(75)90279-5

16. S. Fubini and E. Rabinovici, Nucl. Phys. B **245**, 17 (1984). doi:10.1016/0550-3213(84)90422-X
17. S. J. Brodsky and S. D. Drell, Phys. Rev. D **22**, 2236 (1980). doi:10.1103/PhysRevD.22.2236
18. S. J. Brodsky, D. S. Hwang and I. Schmidt, Phys. Lett. B **530**, 99 (2002) doi:10.1016/S0370-2693(02)01320-5 [hep-ph/0201296].
19. G. F. de Téramond, H. G. Dosch and S. J. Brodsky, Phys. Rev. D **91**, no. 4, 045040 (2015) doi:10.1103/PhysRevD.91.045040 [arXiv:1411.5243 [hep-ph]].
20. H. G. Dosch, G. F. de Téramond and S. J. Brodsky, Phys. Rev. D **91**, no. 8, 085016 (2015) doi:10.1103/PhysRevD.91.085016 [arXiv:1501.00959 [hep-th]].
21. H. G. Dosch, G. F. de Téramond and S. J. Brodsky, Phys. Rev. D **92**, no. 7, 074010 (2015) doi:10.1103/PhysRevD.92.074010 [arXiv:1504.05112 [hep-ph]].
22. T. Liu and B. Q. Ma, Phys. Rev. D **92**, no. 9, 096003 (2015) doi:10.1103/PhysRevD.92.096003 [arXiv:1510.07783 [hep-ph]].
23. S. J. Brodsky and R. F. Lebed, Phys. Rev. D **91**, 114025 (2015) doi:10.1103/PhysRevD.91.114025 [arXiv:1505.00803 [hep-ph]].
24. R. S. Sufian, G. F. de Téramond , S. J. Brodsky, A. Deur and H. G. Dosch, Phys. Rev. D **95**, no. 1, 014011 (2017) doi:10.1103/PhysRevD.95.014011 [arXiv:1609.06688 [hep-ph]].
25. P. A. M. Dirac, Rev. Mod. Phys. **21**, 392 (1949). doi:10.1103/RevModPhys.21.392
26. S. J. Brodsky, H. C. Pauli and S. S. Pinsky, Phys. Rept. **301**, 299 (1998) doi:10.1016/S0370-1573(97)00089-6 [hep-ph/9705477].
27. J. Terrell, Phys. Rev. **116**, 1041 (1959). doi:10.1103/PhysRev.116.1041
28. R. Penrose, Proc. Cambridge Phil. Soc. **55**, 137 (1959). doi:10.1017/S0305004100033776
29. G. Grunberg, Phys. Lett. **95B**, 70 (1980) Erratum: [Phys. Lett. **110B**, 501 (1982)]. doi:10.1016/0370-2693(80)90402-5
30. S. J. Brodsky and H. J. Lu, Phys. Rev. D **51**, 3652 (1995) doi:10.1103/PhysRevD.51.3652 [hep-ph/9405218].
31. S. J. Brodsky, G. F. de Téramond and A. Deur, Phys. Rev. D **81**, 096010 (2010) doi:10.1103/PhysRevD.81.096010 [arXiv:1002.3948 [hep-ph]].
32. A. Deur, V. Burkert, J. P. Chen and W. Korsch, Phys. Lett. B **650**, 244 (2007) doi:10.1016/j.physletb.2007.05.015 [hep-ph/0509113].
33. A. Deur, S. J. Brodsky and G. F. de Téramond, Phys. Lett. B **750**, 528 (2015) doi:10.1016/j.physletb.2015.09.063 [arXiv:1409.5488 [hep-ph]].
34. S. J. Brodsky, G. F. de Téramond , A. Deur and H. G. Dosch, Few Body Syst. **56**, no. 6-9, 621 (2015) doi:10.1007/s00601-015-0964-1 [arXiv:1410.0425 [hep-ph]].
35. D. Binosi, C. Mezrag, J. Papavassiliou, C. D. Roberts and J. Rodriguez-Quintero, Phys. Rev. D **96**, no. 5, 054026 (2017) doi:10.1103/PhysRevD.96.054026 [arXiv:1612.04835 [nucl-th]].
36. K. A. Olive *et al.* [Particle Data Group], Chin. Phys. C **38**, 090001 (2014). doi:10.1088/1674-1137/38/9/090001
37. A. Zee, Princeton, UK: Princeton Univ. Pr. (2010) 576 p
38. M. Mojaza, S. J. Brodsky and X. G. Wu, Phys. Rev. Lett. **110**, 192001 (2013) doi:10.1103/PhysRevLett.110.192001 [arXiv:1212.0049 [hep-ph]].
39. S. J. Brodsky, M. Diehl and D. S. Hwang, Nucl. Phys. B **596**, 99 (2001) doi:10.1016/S0550-3213(00)00695-7 [hep-ph/0009254].
40. J. F. Gunion, S. J. Brodsky and R. Blankenbecler, Phys. Rev. D **8**, 287 (1973). doi:10.1103/PhysRevD.8.287
41. S. J. Brodsky, C. R. Ji and G. P. Lepage, Phys. Rev. Lett. **51**, 83 (1983). doi:10.1103/PhysRevLett.51.83
42. S. J. Brodsky and G. F. de Téramond, arXiv:0901.0770 [hep-ph].
43. S. J. Brodsky and R. F. Lebed, Phys. Rev. Lett. **102**, 213401 (2009) doi:10.1103/PhysRevLett.102.213401 [arXiv:0904.2225 [hep-ph]].
44. A. Banburski and P. Schuster, Phys. Rev. D **86**, 093007 (2012) doi:10.1103/PhysRevD.86.093007 [arXiv:1206.3961 [hep-ph]].
45. S. J. Brodsky and A. Sickles, Phys. Lett. B **668**, 111 (2008) doi:10.1016/j.physletb.2008.07.108 [arXiv:0804.4608 [hep-ph]].
46. F. Arleo, S. J. Brodsky, D. S. Hwang and A. M. Sickles, Phys. Rev. Lett. **105**, 062002 (2010) doi:10.1103/PhysRevLett.105.062002 [arXiv:0911.4604 [hep-ph]].

47. J. W. Cronin, H. J. Frisch, M. J. Shochet, J. P. Boymond, R. Mermod, P. A. Piroue and R. L. Sumner, Phys. Rev. D **11**, 3105 (1975). doi:10.1103/PhysRevD.11.3105
48. D. W. Sivers, S. J. Brodsky and R. Blankenbecler, Phys. Rept. **23**, 1 (1976). doi:10.1016/0370-1573(76)90015-6
49. S. J. Brodsky, Nucl. Part. Phys. Proc. **258-259**, 23 (2015) doi:10.1016/j.nuclphysbps.2015.01.007 [arXiv:1410.0404 [hep-ph]].
50. J. D. Bjorken, S. J. Brodsky and A. Scharff Goldhaber, Phys. Lett. B **726**, 344 (2013) doi:10.1016/j.physletb.2013.08.066 [arXiv:1308.1435 [hep-ph]].
51. D. Ashery, Nucl. Phys. Proc. Suppl. **90**, 67 (2000) [Nucl. Phys. Proc. Suppl. **108**, 321 (2002)] doi:10.1016/S0920-5632(00)00875-6, 10.1016/S0920-5632(02)01354-3 [hep-ex/0008036].
52. P. Wiecki, Y. Li, X. Zhao, P. Maris and J. P. Vary, Phys. Rev. D **91**, no. 10, 105009 (2015) doi:10.1103/PhysRevD.91.105009 [arXiv:1404.6234 [nucl-th]].
53. H. G. Dosch, G. F. de Téramond and S. J. Brodsky, Phys. Rev. D **95**, no. 3, 034016 (2017) doi:10.1103/PhysRevD.95.034016 [arXiv:1612.02370 [hep-ph]].
54. S. J. Brodsky, Few Body Syst. **58**, no. 3, 133 (2017) doi:10.1007/s00601-017-1292-4 [arXiv:1611.07194 [hep-ph]].
55. S. J. Brodsky, Few Body Syst. **57**, no. 8, 703 (2016) doi:10.1007/s00601-016-1070-8 [arXiv:1601.06328 [hep-ph]].
56. S. J. Brodsky, Russ. Phys. J. **60**, no. 3, 399 (2017). doi:10.1007/s11182-017-1089-4
57. E. Klempt and B. C. Metsch, Eur. Phys. J. A **48**, 127 (2012). doi:10.1140/epja/i2012-12127-1
58. M. A. Shifman, World Sci. Lect. Notes Phys. **62**, 1 (1999).
59. S. J. Brodsky, D. S. Hwang, B. Q. Ma and I. Schmidt, Nucl. Phys. B **593**, 311 (2001) doi:10.1016/S0550-3213(00)00626-X [hep-th/0003082].
60. I. Y. Kobzarev and L. B. Okun, Zh. Eksp. Teor. Fiz. **43**, 1904 (1962) [Sov. Phys. JETP **16**, 1343 (1963)].
61. O. V. Teryaev, hep-ph/9904376.
62. V. N. Gribov and L. N. Lipatov, Sov. J. Nucl. Phys. **15**, 438 (1972) [Yad. Fiz. **15**, 781 (1972)].
63. G. Altarelli and G. Parisi, Nucl. Phys. B **126**, 298 (1977). doi:10.1016/0550-3213(77)90384-4
64. Y. L. Dokshitzer, Sov. Phys. JETP **46**, 641 (1977) [Zh. Eksp. Teor. Fiz. **73**, 1216 (1977)].
65. G. P. Lepage and S. J. Brodsky, Phys. Lett. **87B**, 359 (1979). doi:10.1016/0370-2693(79)90554-9
66. G. P. Lepage and S. J. Brodsky, Phys. Rev. D **22**, 2157 (1980). doi:10.1103/PhysRevD.22.2157
67. A. V. Efremov and A. V. Radyushkin, Phys. Lett. **94B**, 245 (1980). doi:10.1016/0370-2693(80)90869-2
68. A. V. Efremov and A. V. Radyushkin, Theor. Math. Phys. **42**, 97 (1980) [Teor. Mat. Fiz. **42**, 147 (1980)]. doi:10.1007/BF01032111
69. H. C. Pauli and S. J. Brodsky, Phys. Rev. D **32**, 1993 (1985). doi:10.1103/PhysRevD.32.1993
70. K. Hornbostel, S. J. Brodsky and H. C. Pauli, Phys. Rev. D **41**, 3814 (1990). doi:10.1103/PhysRevD.41.3814
71. S. J. Brodsky and S. Gardner, Phys. Rev. Lett. **116**, no. 1, 019101 (2016) doi:10.1103/PhysRevLett.116.019101 [arXiv:1504.00969 [hep-ph]].
72. G. F. de Téramond and S. J. Brodsky, Phys. Rev. Lett. **94**, 201601 (2005) doi:10.1103/PhysRevLett.94.201601 [hep-th/0501022].
73. C. Cruz-Santiago, P. Kotko and A. M. Sta?to, Prog. Part. Nucl. Phys. **85**, 82 (2015). doi:10.1016/j.ppnp.2015.07.002
74. K. Y. J. Chiu and S. J. Brodsky, Phys. Rev. D **95**, no. 6, 065035 (2017) doi:10.1103/PhysRevD.95.065035 [arXiv:1702.01127 [hep-th]].
75. S. J. Brodsky, R. Roskies and R. Suaya, Phys. Rev. D **8**, 4574 (1973). doi:10.1103/PhysRevD.8.4574
76. A. Zee, Mod. Phys. Lett. A **23**, 1336 (2008). doi:10.1142/S0217732308027709
77. A. Casher and L. Susskind, Phys. Rev. D **9**, 436 (1974). doi:10.1103/PhysRevD.9.436
78. S. J. Brodsky and R. Shrock, Proc. Nat. Acad. Sci. **108**, 45 (2011) doi:10.1073/pnas.1010113107 [arXiv:0905.1151 [hep-th]].

79. S. J. Brodsky, C. D. Roberts, R. Shrock and P. C. Tandy, Phys. Rev. C **82**, 022201 (2010) doi:10.1103/PhysRevC.82.022201 [arXiv:1005.4610 [nucl-th]].
80. P. P. Srivastava and S. J. Brodsky, Phys. Rev. D **66**, 045019 (2002) doi:10.1103/PhysRevD.66.045019 [hep-ph/0202141].
81. E. P. Verlinde, SciPost Phys. **2**, no. 3, 016 (2017) doi:10.21468/SciPostPhys.2.3.016 [arXiv:1611.02269 [hep-th]].
82. S. Liuti, A. Rajan, A. Courtoy, G. R. Goldstein and J. O. Gonzalez Hernandez, Int. J. Mod. Phys. Conf. Ser. **25**, 1460009 (2014) doi:10.1142/S201019451460009X [arXiv:1309.7029 [hep-ph]].
83. C. Mondal and D. Chakrabarti, Eur. Phys. J. C **75**, no. 6, 261 (2015) doi:10.1140/epjc/s10052-015-3486-6 [arXiv:1501.05489 [hep-ph]].
84. C. Lorce, B. Pasquini and M. Vanderhaeghen, JHEP **1105**, 041 (2011) doi:10.1007/JHEP05(2011)041 [arXiv:1102.4704 [hep-ph]].
85. S. J. Brodsky, AIP Conf. Proc. **1105**, 315 (2009) doi:10.1063/1.3122202 [arXiv:0811.0875 [hep-ph]].
86. S. J. Brodsky, Nucl. Phys. A **827**, 327C (2009) doi:10.1016/j.nuclphysa.2009.05.068 [arXiv:0901.0781 [hep-ph]].
87. S. J. Brodsky, D. S. Hwang and I. Schmidt, Phys. Lett. B **530**, 99 (2002) doi:10.1016/S0370-2693(02)01320-5 [hep-ph/0201296].
88. S. J. Brodsky, P. Hoyer, N. Marchal, S. Peigne and F. Sannino, Phys. Rev. D **65**, 114025 (2002) doi:10.1103/PhysRevD.65.114025 [hep-ph/0104291].
89. S. J. Brodsky, B. Pasquini, B. W. Xiao and F. Yuan, Phys. Lett. B **687**, 327 (2010) doi:10.1016/j.physletb.2010.03.049 [arXiv:1001.1163 [hep-ph]].
90. S. J. Brodsky, D. S. Hwang, Y. V. Kovchegov, I. Schmidt and M. D. Sievert, Phys. Rev. D **88**, no. 1, 014032 (2013) doi:10.1103/PhysRevD.88.014032 [arXiv:1304.5237 [hep-ph]].
91. S. J. Brodsky and H. J. Lu, Phys. Rev. Lett. **64**, 1342 (1990). doi:10.1103/PhysRevLett.64.1342
92. S. J. Brodsky, I. Schmidt and J. J. Yang, Phys. Rev. D **70**, 116003 (2004) doi:10.1103/PhysRevD.70.116003 [hep-ph/0409279].
93. I. Schienbein, J. Y. Yu, C. Keppel, J. G. Morfin, F. Olness and J. F. Owens, Phys. Rev. D **77**, 054013 (2008) doi:10.1103/PhysRevD.77.054013 [arXiv:0710.4897 [hep-ph]].